JOURNAL OF SOLID STATE CHEMISTRY 70, 262–270 (1987)

The Antiferromagnetic Structures of $KFeS_2$, $RbFeS_2$, $KFeSe_2$, and $RbFeSe_2$ and the Correlation between Magnetic Moments and Crystal Field Calculations*

W. BRONGER, A. KYAS, AND P. MÜLLER

Institut für Anorganische Chemie der RWTH Aachen, Prof.-Pirlet-Strasse 1, 5100 Aachen, Federal Republic of Germany

Received December 5, 1986

The ternary compounds $KFeS_2$, $RbFeS_2$, $KFeSe_2$, and $RbFeSe_2$ were prepared and their crystal structures were determined from single-crystal diffractometer data. The atomic arrangement in the isotypic compounds (space group $C2/c$) is characterized by tetrahedra of chalcogen atoms. Those tetrahedra are centered by iron ions and linked by edges, thus forming chains of $^1_\infty[FeX_{4/2}]$ frameworks ($X \triangleq$ S or Se). Susceptibility measurements are reported. Neutron diffraction experiments on powdered samples revealed magnetic structures in the antiferromagnetically ordered state. The magnetic moments of the iron ions shows a significant dependence of the atomic arrangement. Therefore calculations based on a simple point charge model are discussed to correlate the magnetic moments and crystal field splittings. © 1987 Academic Press, Inc.

Introduction

$KFeS_2$ has been known since 1869 (*1, 2*). Crystals of $KFeS_2$ were obtained from the reaction of a mixture of potassium carbonate, iron, and sulfur, followed by extracting the solidified melt with water. The structure was first determined in 1942 by Boon and MacGillavry (*3*).

$RbFeS_2$ and $CsFeS_2$ were first prepared and their structures determined in 1968 (*4*). Since then the analogous selenium compounds have been prepared, too; up to now only powder data have been available for the investigation of their crystal structures (*5*).

The magnetic properties of these alkali chalcogenoferrates are characterized by antiferromagnetic interactions of the iron ions. They have been the subject matter of several publications based on susceptibility measurements and Mössbauer spectra (*4, 6–12*). Hereafter the results of further experiments concerning $KFeS_2$, $RbFeS_2$, $KFeSe_2$, and $RbFeSe_2$ are reported. First, detailed single-crystal X-ray data and powder neutron diffraction data are given. Finally, the series of magnetic moments is explained by means of the crystal field theory. Thus a further insight in bonding properties is gained.

Preparation

The compounds $KFeS_2$ and $RbFeS_2$ were prepared by the reaction of a mixture of alkali carbonate and iron sponge in the molar ratio 4 : 1 in a stream of purified H_2S for

* Dedicated to Dr. H. Nowotny.

0022-4596/87 $3.00

4 hr at 1000 K (*13*). The potassium carbonate was obtained by dehydration of $K_2CO_3 \cdot 1.5\ H_2O$ (Alfa-Ventron, ultrapure) in a stream of argon at 420 K. For the rubidium carbonate (Alfa-Ventron) a purity of 99.9% is specified, for the iron sponge (Zimsser) 99.96%. The H_2S (Gerling, Holz & Co., purity 99.85%) was dried with calcium chloride and phosphorus(V) oxide.

The mixture of alkali carbonate and iron sponge was placed into a corundum boat and then into a quartz tube which was heated up to 1000 K. After the reaction the sample was cooled for 8 hr in an H_2S atmosphere. Extraction of the solidified melt with water and alcohol yielded well-developed violet needles. Quenching of the samples led to very small crystals, the physical properties of which did not differ from those cooled slowly. Those small crystals were preferred for the experiments with powdered samples. As $KFeS_2$ and $RbFeS_2$ are not stable when exposed to air for any considerable length of time, they were stored under argon.

The selenides $KFeSe_2$ and $RbFeSe_2$ were prepared in an analogous manner. The reaction was carried out at 1050 K in a stream of hydrogen and gaseous selenium. For the hydrogen gas (Fa. Linde) as well as for the selenium powder (Johnson Matthey Ltd.), a purity of 99.999% is specified. The reaction products were extracted with water and alcohol, dried under vacuum, and stored under argon. Violet needle-shaped crystals similar to the sulfides were formed.

Structure Determination

The crystal structures of the alkali iron chalcogenides $AFeX_2$ ($A \triangleq$ K or Rb, $X \triangleq$ S or Se) were determined by X-ray experiments on single crystals. The measurements were performed with a computer-controlled single-crystal diffractometer (Nonius CAD4, graphite monochromator). All calculations were carried out using a PDP 11/45 computer with programs of the Nonius SDP system. The results of the final calculations are given in Table I. Table II shows the lattice constants, determined by X-ray diffraction on powdered samples (Guinier–Simon method, $CuK\alpha_1$ radiation, α-quartz as standard).

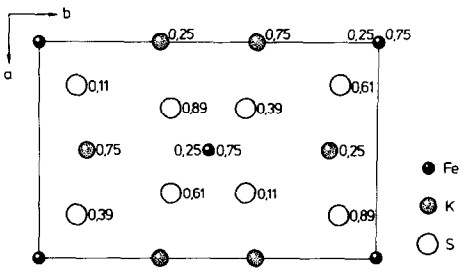

FIG. 1. Atomic arrangement of $KFeS_2$.

The four compounds are isotypic and crystallize in the monoclinic $KFeS_2$ type (space group $C2/c$, $Z = 4$). The atomic arrangement is shown in Fig. 1. It is characterized by one-dimensionally edge-linked sulfur tetrahedra centered by the iron atoms. The $^1_\infty[FeS^-_{4/2}]$ chains along the c direction are separated by the alkali atoms. Table III shows the shortest atomic distances and the X–Fe–X angles in the chains.

Susceptibility Measurements

Magnetic susceptibilities of the compounds $KFeS_2$, $RbFeS_2$, $KFeSe_2$, and $RbFeSe_2$ were determined by the Faraday method in the temperature range of 3.7–295 K. The samples were sealed in ampoules made from synthetic quartz. The measurements at different magnetic field strengths (4×10^5–11×10^5 Am^{-1}) showed that susceptibilities depended little on field strength. The χ_{mol}–T diagram (Fig. 2) is based exclusively on values obtained at the strongest field. Diamagnetism was corrected by adding the sum of the ionic increments (*14*).

The small positive values of the magnetic

TABLE I

X-RAY EXPERIMENTS ON SINGLE CRYSTALS: RADIATION, 2θ RANGE, NUMBER OF SYMMETRY-INDEPENDENT REFLECTIONS WITH $F_0^2 \geq 3\,\sigma\,(F_0^2) \triangleq Z(F_0^2)$, R VALUES, ATOMIC COORDINATES, AND THERMAL PARAMETERS U_{ij} (10^{-4} Å^2)[a]

	$KFeS_2$	$RbFeS_2$	$KFeSe_2$	$RbFeSe_2$
Radiation	Mo$K\alpha$	Mo$K\alpha$	Ag$K\alpha$	Ag$K\alpha$
2θ range	$1 \leq \theta \leq 35$	$1 \leq \theta \leq 26$	$1 \leq \theta \leq 24$	$1 \leq \theta \leq 24$
$Z(F_0^2)$	573	337	290	320
R value	0.03	0.051	0.075	0.031
Fe in 4*e*				
x	0.0	0.0	0.0	0.0
y	0.99668(8)	0.9976(3)	−0.0031(6)	−0.0021(2)
z	0.25	0.25	0.25	0.25
U_{11}	176(2)	160(10)	130(20)	217(9)
U_{22}	193(3)	230(10)	150(30)	190(10)
U_{33}	114(2)	79(8)	210(20)	150(8)
U_{12}	0	0	0	0
U_{13}	64(2)	53(7)	70(20)	96(6)
U_{23}	0	0	0	0
A in 4*e*				
x	0.0	0.0	0.0	0.0
y	0.3572(1)	0.3553(2)	0.3608(10)	0.3585(2)
z	0.25	0.25	0.25	0.25
U_{11}	283(5)	237(8)	380(50)	263(7)
U_{22}	291(6)	300(10)	240(60)	291(8)
U_{33}	270(5)	210(7)	340(50)	255(7)
U_{12}	0	0	0	0
U_{13}	62(4)	56(6)	140(40)	111(5)
U_{23}	0	0	0	0
X in 8*f*				
x	0.1960(2)	0.1905(6)	0.2012(5)	0.1948(2)
y	0.1098(1)	0.1061(4)	0.1136(3)	0.1130(1)
z	0.1068(2)	0.0981(7)	0.1099(6)	0.1018(2)
U_{11}	247(3)	250(10)	250(10)	266(4)
U_{22}	239(4)	250(20)	240(10)	249(5)
U_{33}	172(3)	160(10)	219(9)	194(4)
U_{12}	−82(3)	−80(10)	−100(20)	−81(5)
U_{13}	93(2)	70(10)	113(7)	128(3)
U_{23}	−28(3)	−20(10)	−30(20)	−38(5)

Note. Standard deviations are given in parentheses.

[a] The anisotropic temperature factor is defined as $\exp[-2\pi^2(U_{11}h^2a^{*2} + U_{22}k^2b^{*2} + \cdots + 2U_{23}klb^*c^*)]$.

susceptibilities indicate antiferromagnetic interactions. There is nothing in these measurements to connect temperatures with three-dimensional magnetic ordering, as shown by Mössbauer spectra (*9, 10*). This can be explained by the change of a one-dimensionally to a three-dimensionally ordered spin arrangement, consistent with a chain structure. A transition of this kind does not lead to a significant maximum in

TABLE II

LATTICE CONSTANTS DETERMINED BY THE GUINIER METHOD

	$KFeS_2$	$RbFeS_2$	$KFeSe_2$	$RbFeSe_2$
a(Å)	7.084(3)	7.223(3)	7.342(2)	7.474(2)
b(Å)	11.303(4)	11.725(3)	11.746(2)	12.091(3)
c(Å)	5.394(2)	5.430(2)	5.629(1)	5.662(2)
β(°)	113.2(1)	112.0(1)	113.52(2)	112.38(2)

the χ_{mol}–T diagram, such as is found when an unordered paramagnetic state changes into an antiferromagnetically ordered one. On the other hand, a three-dimensional magnetic ordering causes a hyperfine splitting in the Mössbauer spectrum and sharp Bragg reflections in neutron diffraction.

Neutron Diffraction Experiments

For these experiments powdered samples were filled into aluminum tubes of 40 mm in length and 8 mm in diameter. The experiments were carried out with the powder diffractometer of the BER II at the

TABLE III

INTERATOMIC DISTANCES (Å) AND ANGLES (°)

	$KFeS_2$	$RbFeS_2$	$KFeSe_2$	$RbFeSe_2$
	Distances and angles in a FeX_4 tetrahedron			
Fe–X (2×)	2.231(2)	2.235(5)	2.363(5)	2.365(2)
Fe–X (2×)	2.237(2)	2.246(5)	2.369(6)	2.367(2)
Fe–Fe (2×)	2.698(1)	2.716(1)	2.815(1)	2.832(1)
X–X (2×)	3.561(3)	3.564(9)	3.803(7)	3.790(3)
X–X	3.671(4)	3.701(9)	3.865(8)	3.875(3)
X–X (2×)	3.665(2)	3.683(6)	3.879(5)	3.890(2)
X–X	3.756(5)	3.751(8)	3.949(6)	3.939(2)
X–Fe–X	105.70(5)	105.4(1)	107.0(1)	106.48(4)
	114.69(9)	114.1(3)	113.4(3)	112.8(1)
	110.26(8)	110.5(2)	110.1(1)	110.60(6)
	Further distances			
A–X (2×)	3.306(4)	3.436(5)	3.403(3)	3.527(2)
A–X (2×)	3.345(2)	3.456(5)	3.488(11)	3.572(3)
A–X (2×)	3.427(3)	3.459(5)	3.543(4)	3.574(2)
A–X (2×)	3.475(2)	3.598(5)	3.588(10)	3.704(3)
X–X	3.557(3)	3.735(9)	3.608(7)	3.761(3)
A–Fe (2×)	3.876(4)	3.978(2)	3.993(6)	4.100(2)
A–Fe (2×)	3.877(2)	4.005(4)	4.004(6)	4.116(2)
A–Fe	4.075(2)	4.194(4)	4.274(14)	4.360(4)
A–A (2×)	4.207(2)	4.346(4)	4.315(18)	4.441(4)
A–A (2×)	4.262(4)	4.378(5)	4.464(14)	4.562(3)

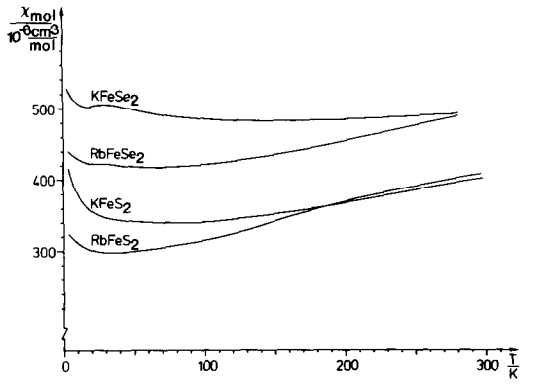

FIG. 2. Temperature dependence of the magnetic susceptibilities of the compounds $AFeX_2$.

Hahn–Meitner Institut in Berlin. Neutron diffraction diagrams were recorded by a position sensitive detector in a 2θ range of 80° with a resolution of 0.2° (λ = 2.39 Å, collimation 10′). Low temperatures were achieved using a closed-cycle refrigerator. High temperatures were kept constant throughout the sample by short-circuiting its far end to the oven using a copper heat conductor.

Table IV contains the results of the neutron diffraction experiments. The Néel temperatures observed in Mössbauer spectra are taken from the literature. Neutron diffraction diagrams measured above the Néel temperatures show only those intensities of Bragg reflections which are due to nuclear scattering. Profile-fitting calculations after the Rietveld method were in agreement with the measured profile. Starting values for the refinement were taken from single-crystal X-ray experiments. The neutron diffraction diagrams at the lowest temperatures showed changes from the intensities of reflections observed at high temperatures; and in addition they showed reflections which did not follow the crystallographic extinction $h0l$ only with $l = 2n$. These additional reflections can only be explained by a spin structure with ferromagnetic ordering in the a–b plane and antiferromagnetic ordering along the c axis. Calculations based on this model led to the parameters given in Table IV after the refinement through Rietveld's program (*15*).

For the sulfides a spin structure characterized by spins in the a–c plane forming an angle of 20° with the c axis is obtained. In the selenides the spins are aligned parallel to the b axis. This means that the sulfides belong to the Shubnikov group $C2'/c$, and the selenides to $C2/c'$. Figure 3 shows the two spin structures. The components of the magnetic moments projected to the crystallographic axis and the resulting magnetic moments according to the formula $\mu = 2S\mu_B$ are given in Table IV. Previously published $KFeS_2$ neutron diffraction data are in agreement with our results (*16, 17*).

Magnetic Moments and Crystal Field Calculations

The magnetic moments of the iron atoms in the antiferromagnetic structures of $KFeS_2$, $RbFeS_2$, $KFeSe_2$, and $RbFeSe_2$ show significant deviations from the value expected for a d^5 ion with $\mu = 5.0\ \mu_B$ (see Table IV). Obviously spin states with S = 3/2 and S = 1/2 play an important part.

Our earlier investigations into the magnetic properties of the ternary sulfide $CsFeS_2$ revealed low spin states of iron ions. After mechanically destroying linear

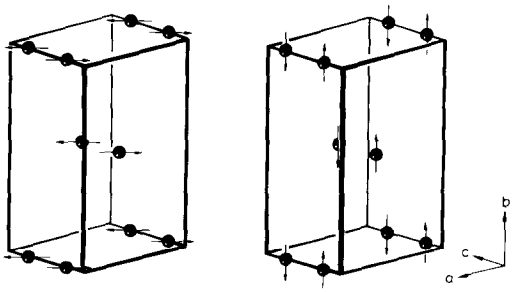

FIG. 3. Spin structures of $AFeS_2$ (left side, space group $C2'/c$) and of $AFeSe_2$ (right side, space group $C2/c'$).

TABLE IV

NEUTRON DIFFRACTION EXPERIMENTS: SPACE GROUPS, NÉEL TEMPERATURES, PARAMETERS AFTER PROFILE REFINEMENT, AND R VALUES

	$KFeS_2$		$RbFeS_2$		$KFeSe_2$		$RbFeSe_2$	
T (K):	295	11	295	11	393	15	295	14
Space group	$C2/c$	$C2'/c$	$C2/c$	$C2'/c$	$C2/c$	$C2/c'$	$C2/c$	$C2/c'$
Néel temp. (K)	250(1) (Ref. (9))		188(1) (Ref. (9))		310(1) (Ref. (10))		249(1) (Ref. (10))	
a(Å)	7.082(4)	7.028(4)	7.245(3)	7.189(2)	7.369(2)	7.278(2)	7.450(2)	7.389(1)
b(Å)	11.329(4)	11.201(5)	11.762(4)	11.619(5)	11.796(4)	11.611(4)	12.056(3)	11.918(2)
c(Å)	5.403(3)	5.388(2)	5.455(2)	5.435(2)	5.639(2)	5.615(2)	5.644(1)	5.629(1)
β(Å)	113.2(1)	113.3(1)	112.0(1)	112.2(1)	113.5(1)	113.7(1)	112.39(1)	112.55(1)
$B_{overall}$(Å^2)	0.7(5)	0.4(4)	1.1(4)	0.2(4)	5.0(3)	0.4(4)	0.9(4)	0.6(3)
A in 4e								
x	0.0	0.0	0.0	0.0	0.0	0.0	0.0	0.0
y	0.359(3)	0.350(5)	0.355(2)	0.354(2)	0.370(3)	0.362(4)	0.3560(21)	0.3596(12)
z	0.25	0.25	0.25	0.25	0.25	0.25	0.25	0.25
Fe in 4e								
x	0.0	0.0	0.0	0.0	0.0	0.0	0.0	0.0
y	0.002(2)	−0.001(2)	0.0	0.0	−0.011(2)	−0.017(2)	0.0052(13)	−0.0010(9)
z	0.25	0.25	0.25	0.25	0.25	0.25	0.25	0.25
X in 8f								
x	0.186(5)	0.198(5)	0.209(4)	0.189(5)	0.181(3)	0.169(3)	0.1950(18)	0.1992(10)
y	0.109(2)	0.115(3)	0.103(2)	0.110(2)	0.115(1)	0.108(1)	0.1093(12)	0.1105(6)
z	0.123(6)	0.122(6)	0.100(9)	0.070(11)	0.104(3)	0.110(3)	0.0969(35)	0.1056(25)
$\mu_{x,Fe}$ (μ_B)		0.85(21)		0.6(4)		0.0		0.0
$\mu_{y,Fe}$ (μ_B)		0.0		0.0		3.0(2)		2.66(5)
$\mu_{z,Fe}$ (μ_B)		−1.47(17)		−1.4(6)		0.0		0.0
μ_{Fe} (μ_B)		1.9(3)		1.8(3)		3.0(2)		2.66(5)
R	0.062	0.056	0.069	0.065	0.037	0.076	0.056	0.043
R_{nuci}		0.05		0.061		0.068		0.038
R_{magn}		0.108		0.127		0.124		0.101

magnetic interactions in the $^1_\infty[FeS_{4/2}^-]$ chains of $CsFeS_2$, the iron ion was found to be in a low spin state. Furthermore in mixed crystals of $CsGa_{1-y}Fe_yS_2$ measurements of magnetic susceptibilities pointed to a low spin configuration of Fe^{3+} (*6*). This conforms to the low magnetic hyperfine splitting in the Mössbauer spectrum pointing to nearly complete spin pairing (*9*).

These anomalous magnetic moments of transition metal ions observed here in the tetrahedral holes of a framework structure can be explained by means of the crystal field theory. This theory becomes applicable mainly for the reason that in the ternary alkali transition metal chalcogenides $A_xM_yX_z$ the strong electropositive alkali metal atoms build up a pressure of electrons, thus forming complex $[M_yX_z]^{x-}$ anions. Therefore a three-dimensional delocalization of electronic states loses some of its importance. When x is increased, thereby raising the electronic pressure in the lattice, disintegration of the $[M_yX_z]^{x-}$ frameworks in the ternary compounds $A_xM_yX_z$ is to be expected (*18*). The chalcogenides $AFeX_2$ discussed here contain one-dimensional $[FeS_2]^-$ and $[FeSe_2]^-$ chains of edge-linked tetrahedra, Na_3FeS_3 (*19*) $[Fe_2S_6]^{6-}$ double tetrahedra, and finally

Na_5FeS_4 (*20*), which is richest in alkali metal isolated $[FeS_4]^{5-}$ tetrahedra. We will include the isolated $[Fe_yS_z]^{x-}$ groups together with the chain structures when discussing the results of our crystal field calculations to achieve an extended model. As a first step in a perturbation calculation the oxidation numbers of the atoms concerned were taken as point charges to assess the influence of the coordinating atoms on the electronic states of the central iron atom. Details of this procedure, which follows the strong field method, have been described in various papers. (*18, 21, 22*).

In Fig. 4a the energy splittings of the *d* orbitals of a Fe^{3+} ion are shown, first, in a regular tetrahedral coordination of S^{2-} anions, and second, in real coordination, which is found in Na_5FeS_4 and includes only the four nearest sulfur atoms ($r < 2.3$ Å). Further splittings are pointed out, including the influence of all ions up to the specified radius *r* around the central atom. The result shows that ions farther away than the first ligand sphere essentially do not change the splitting of the *d* orbitals. The $[FeS_4]^{5-}$ tetrahedra can be regarded as swimming in a sea of sodium ions. This situation is quite similar to that of a solution of complex ions.

When computing analogous diagrams for the structure of Na_3FeS_3 the picture changes drastically (cf. Fig. 4b). In this case the Fe^{3+} ion occupying the neighboring tetrahedral hole in the $[Fe_2S_6]^{6-}$ unit at a distance <3.0 Å exercises a powerful influence on the energy splitting of the *d* orbitals. This influence is diminished with regard to those ions which are farther away from the central atom (up to 5.4, 8.0 Å); the remaining energy splitting; however, is distinctly larger than that arrived at for the isolated tetrahedron (Fig. 4a). The influence of a higher number of atoms than those belonging to the first ligand sphere is even more prominent in the chain structures of the compounds $KFeS_2$, $RbFeS_2$, $KFeSe_2$, and $RbFeSe_2$ (cf. Fig. 4c). Those *d* states participating in the *z* direction are accordingly reduced in energy, as the positive charges of the iron atoms are arranged at a relative short distance in the same direction, i.e., along the chain.

In Fig. 5 the results of the crystal field calculations are compared. In the series of splitting diagrams there is an unmistakable correlation of the measured magnetic moments and the energies computed on a relative scale. Small energy splittings as calculated for Na_5FeS_4 correspond to a magnetic

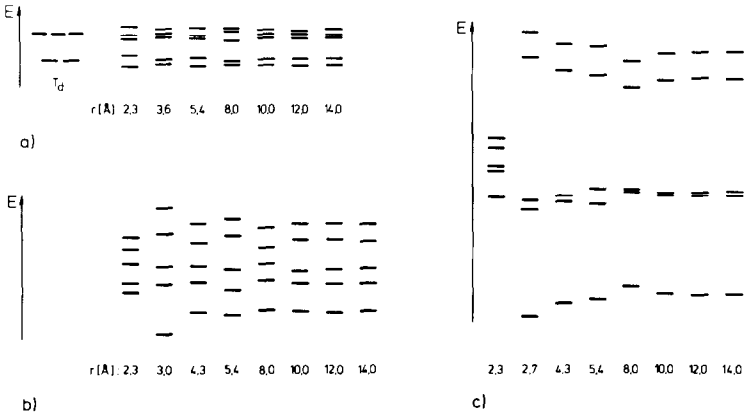

FIG. 4. Energy splittings in dependence of point-charge model calculations including different numbers of ions. (a) Na_5FeS_4, (b) Na_3FeS_3, (c) $KFeS_2$.

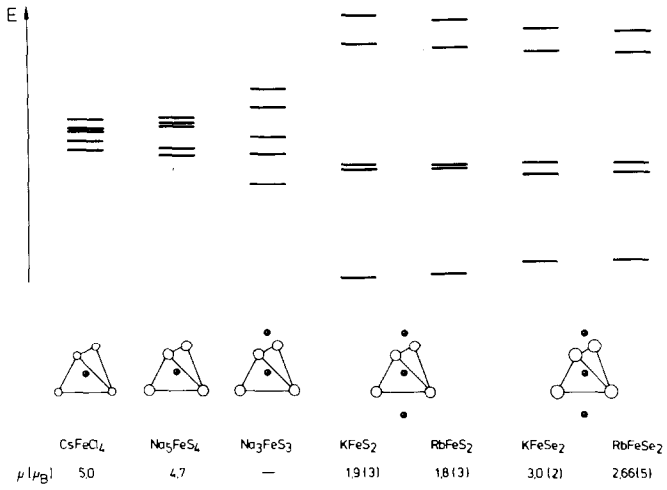

FIG. 5. Energy splittings in comparison with the magnetic moments.

moment for the Fe^{3+} ion approaching a high spin value. In the case of the largest energy splittings, calculated for $KFeS_2$ and $RbFeS_2$, the moments were found to be spread between a low spin value ($S = 1/2$) and a medium spin value ($S = 3/2$). The chain structures of the selenides follow the same pattern. The computed energy splittings are smaller than those for the sulfides, but distinctly larger than for an isolated tetrahedron. Thus magnetic moments larger than those in the sulfides but smaller than a high spin value are to be expected. Neutron diffraction experiments confirm this. For the compound Na_3FeS_3 we have as yet not been able to determine the magnetic moments from neutron diffraction experiments; nevertheless a magnetic moment distinctly smaller than 5.0 μ_B is to be expected.

The use of oxidation numbers as point charges in our calculations naturally leads to a maximum value of energy splittings. Analogous calculations with reduced point charges showed smaller splittings as was to be expected. Nevertheless the relative sequence discussed is valid.

The increase of Fe–S distances in the isolated $[FeS_4]^{5-}$ group with regard to those in the $[FeS_2]^-$ chains corresponds to the series of magnetic moments: For iron ions in the low spin state a smaller radius than for those in the high spin state is to be expected.

The deviations of the measured magnetic moments from those calculated for the different spin states can be explained by the neglect of interelectronic interactions and spin-orbit coupling. Interactions of excited states with ground states may be responsible for the deviations from spin-only values.

In Fig. 5 the halogenide $CsFeCl_4$ (*23*) is alongside the chalcogenides. Susceptibility measurements have revealed a magnetic moment equaling the spin-only value for a Fe^{3+} ion with five unpaired electrons. This compound contains isolated $[FeCl_4]^-$ anions; their spectroscopic data as measured in solution are available. In the literature a ΔE value for the splitting of the e and t_2 state of about 5000 cm^{-1} is quoted (*14*). Transferring this value into the series of splittings in Fig. 5, spin-pairing can be expected for those compounds with linked tetrahedra. Spectroscopic investigations

will be carried out in due course. However, the above-mentioned relative calculations already convey a detailed picture which also has been observed in a series of ternary manganese compounds (*21, 24*).

Some months ago extended Hückel calculations for the $[FeS_2]^-$ chains of our compounds were published by Silvestre and Hoffmann (*25*). With regard to the splitting of *d* orbitals their analysis is not inconsistent with our results. The advantage of the model as described above is that it produces information on local properties in a simple approximation, thus allowing predictions with regard to other compounds.

Acknowledgments

The authors express their thanks to Mr. K. Kruse for performing the single-crystal diffraction experiments. Thanks are also due to Prof. Dr. H. Dachs for giving access to the multicounter at the BER II in the Hahn–Meitner Institut in Berlin. Moreover, we are grateful to the Bundesminister für Forschung und Technologie and the Fonds der Chemischen Industrie for financial support.

References

1. K. PREIS, *J. Prakt. Chem.* **107,** 12 (1869).
2. R. SCHNEIDER, *J. Prakt. Chem.* **108,** 16 (1869).
3. J. W. BOON, AND C. H. MACGILLAVRY, *Rec. Trav. Chim. Pays-Bas* **61,** 910 (1942).
4. W. BRONGER, *Z. Anorg. Allg. Chem.* **359,** 225 (1968).
5. W. BRONGER, *Naturwissenschaften* **53,** 525 (1966).
6. W. BRONGER, AND P. MÜLLER, *J. Less-Common Met.* **70,** 253 (1980).
7. P. MÜLLER, dissertation, Technische Hochschule Aachen (1980).
8. A. KYAS, dissertation, Technische Hochschule Aachen (1981).
9. H. P. NISSEN, AND K. NAGORNY, *Z. Phys. Chem. NF* **95,** 301 (1975).
10. H. P. NISSEN, AND K. NAGORNY, *Z. Phys. Chem. NF* **99,** 14 (1976).
11. W. V. SWEENEY, AND R. E. COFFMAN, *Biochim. Biophys. Acta* **286,** 26 (1972).
12. D. C. JOHNSTON, S. C. MRAW, AND A. J. JACOBSON, *Solid State Comm.* **44,** 255 (1982).
13. D. SCHMITZ, AND W. BRONGER, *Naturwissenschaften* **58,** 322 (1971).
14. A. WEISS, AND H. WITTE, "Magnetochemie," Verlag-Chemie, Weinheim (1973).
15. H. M. RIETVELD, *J. Appl. Crystallogr.* **2,** 65 (1969).
16. T. TOMKOWICZ, A. SZYTULA, AND H. BAK-PTASIEWICZ, *Phys. Status. Solidi A* **57,** K25 (1980).
17. M. NISHI, AND Y. ITO, *Solid State Commun.* **30,** 571 (1979).
18. W. BRONGER, AND P. MÜLLER, *J. Less-Common Met.* **100,** 241 (1984).
19. P. MÜLLER, AND W. BRONGER, *Z. Naturforsch. B* **34,** 1264 (1979).
20. K. O. KLEPP, AND W. BRONGER, *Z. Anorg. Allg. Chem.* **532,** 23 (1986).
21. W. BRONGER, *Pure Appl. Chem.* **57,** 1363 (1985).
22. A. L. COMPANION, AND M. A. KOMARYNSKY, *Chem. Educ.* **41,** 257 (1964).
23. G. MEYER, *Z. Anorg. Allg. Chem.* **436,** 87 (1977).
24. W. BRONGER, R. HÖPPNER, P. MÜLLER, AND H.-U. SCHUSTER, *Z. Anorg. Allg. Chem.* **539,** 175 (1986).
25. J. SILVESTRE, AND R. HOFFMANN, *Inorg. Chem.* **24,** 4108 (1985).